Displacement Damage-induced catastrophic second breakdown in silicon carbide Schottky power diodes

Leif Scheick, *Member, IEEE*, Luis Selva, Heidi Becker

Abstract—A novel catastrophic breakdown mode in reverse biased silicon carbide diodes has been seen for particles that are too low in LET to induce SEB, however SEB-like events were seen from particles of higher LET. The low LET breakdown mechanism correlates with second breakdown in diodes due to increased leakage and assisted charge injection from incident particles. Percolation theory was used to predict some basic responses of the devices.

I. Introduction

Silicon carbide devices are becoming more attractive for harsh environments due to the inherent toughness of the silicon carbide substrate. Due to the wide energy band gap, silicon carbide devices can operate at extremely high temperatures without intrinsic conduction effects. Silicon carbide can endure an electric field about eight times greater than silicon or GaAs before exhibiting avalanche breakdown. High breakdown electric fields allow for very high-voltage, high-power devices such as power diodes. Also, devices can be scaled aggressively, providing ULSI options for integrated circuits. Silicon carbide has a high thermal conductivity. Heat will flow more freely through silicon carbide than other semiconductor materials and most metals at room temperature. This property allows extremely high power level operation and the dissipation of the generated energy. The wide band gap also gives silicon carbide good resistance to lattice damage, especially from displacement damage. Also, the wide band gap of silicon carbide corresponds to unique optical properties, which have been utilized in the fabrication of blue and green LEDs. 4H-SiC has a band gap energy of 3.26 eV and 6H-SiC has a band gap energy of 3.03 eV. In comparison, GaAs has a band gap energy of 1.43 eV and silicon has a band gap energy of 1.12 eV. Table I compares these and other material properties.

Silicon carbide devices are used in a wide variety of applications and have been studied for radiation effects and reliability in a wide spectrum of environments [1]-[3]. The innate robustness of silicon carbide gives it a high breakdown voltage and resistance to stress induced breakdown [4]-[7]. Silicon carbide has recently been studied for total ionizing and displacement damage effects [8]-[12]. Silicon carbide has shown innate hardness to displacement damaging and ionizing radiation. Discrete silicon carbide devices have shown a similar robustness in performance during and after irradiation. This paper presents and discusses catastrophic failure modes in silicon carbide power diodes due to proton and heavy ion radiation that contradicts the current body of results.

TABLE I.
COMPARISON OF SEMICONDUCTOR PARAMETERS.

	4H-SiC	6H-SiC	GaAs	Silicon
Band gap energy [eV]	3.26	3.03	1.43	1.12
Breakdown electric field [V/cm]	2.2E+06	2.4E+06	3.0E+05	2.4E+05
Thermal Conductivity [W/cm K @ RT]	3.45	3.45	0.5	1.5
Saturates electron drift velocity [cm/sec (@ E 2 x 10^5 V/cm)]	2E+07	2E+07	1E+07	1E+07

II. Theory

Silicon carbide Schottky diodes have been available commercially for some time. Schottky diodes have been shown to be simple to manufacture and the Schottky architecture has been shown to be very compatible with the silicon carbide substrate. Silicon carbide's lattice structure allows for unique doping structure. Nitrogen doping takes a carbon site and aluminum takes the silicon site. This characteristic allows for compensated doping and more defined intrinsic regions [4]-[6].

Figure 1 juxtaposes a pn diode structure and a Schottky diode structure. The primary difference is that the pn diode is a minority carrier device and the Schottky diode is a majority carrier device. The rectifying structure in the pn diode is the pn depletion region, while the Schottky diode uses a metal semiconductor contact as the rectifying junction. The breakdown characteristics are essentially the same for pn and Schottky diodes. Silicon Schottky diodes have lower breakdown voltages compared to similar silicon pn diodes due to high curvature in depletion region layers, silicon surface effects, and ohmic contact issues [4]-[6]. Device architecture can compensate for some of the weaknesses of Schottky structures. Silicon carbide's wide band gap, and therefore higher breakdown voltage, allows for a more robust Schottky device.

Silicon carbide has many traits that lead to reliability challenges. First, silicon carbide lattices continue to suffer from a variety of defect producing impurities [13]. Silicon carbide can experience burnout due to defects in the lattice and breakdown characteristics continue to be a limiting factor in silicon carbide devices [13]. Screw plane defects can cause microfilaments that lead to device breakdown. Large screw defects, with Burg vectors over two lattice sites, are called micro-pipes and are a major failure mode in silicon carbide substrates [13], [14]. Micropipes and voids in silicon carbide are very conductive, which causes silicon carbide power devices to be less reliable. Silicon carbide also has a higher

[1] The research in this paper was carried out at the Jet Propulsion Laboratory, California Institute of Technology under contract with the National Aeronautics and Space Administration (NASA) Code AE, under the Electronic Parts and Packaging Program (NEPP).
L. Scheick is with the Jet Propulsion Laboratory, California Institute of Technology, Pasadena, CA 91109 USA (telephone: 818-354-3272, e-mail: leif.scheick@jpl.nasa.gov).
H. Becker is with the Jet Propulsion Laboratory, California Institute of Technology, Pasadena, CA 91109 USA (telephone: 818-353-5491, e-mail: heidi.becker@jpl.nasa.gov).
L. Selva is with the Jet Propulsion Laboratory, California Institute of Technology, Pasadena, CA 91109 USA (telephone: 818-354-5751, e-mail: luis.selva@jpl.nasa.gov).

propensity to negative temperature coefficient breakdown in the presence of defects. Silicon and silicon carbide have a 20% lattice mismatch. The transition from silicon to silicon carbide, as in poorly made crystals with areas of only silicon, can cause defects and stresses on the substrate [15].

Second, silicon carbide exhibits "polytypism," which makes fabrication and process control a uniquely hard challenge for silicon carbide devices. Multiple types in a substrate can lead to plane, point and screw defects in a substrate [7], [13]. These defects decrease the breakdown voltage of silicon carbide. Neutron irradiation has been shown to induce defects in silicon carbide substrates [15]. The physical structure and response of cascades from energetically displaced Si atoms have been investigated [16]-[17]. These investigations have shown that irradiated silicon carbide can exhibit clusters of defects tens of nanometers in size.

Silicon carbide has exhibited several reliability problems that have seriously impacted yield. Figure 2, taken from [18], plots the distribution of breakdown voltages of virgin Schottky barrier diodes. These diodes were free of micropipe defects, which are a major cause of failure in silicon carbide. Lesser defects are present and presumably contribute to the breakdown variation. Since defect density has been correlated with lower breakdown voltages, defects induced by radiation are expected to lower breakdown voltage and the determination of this response is a primary focus of this study.

All diodes exhibit a high current, low voltage condition after avalanche breakdown that is related to the thermal breakdown of the device. This is called second breakdown or snap back. The second breakdown condition onsets when the intrinsic carrier concentration, n_i, is equal to the dopant concentration, $N_{n,p}$, or

$$n_i = N_{n,p} \text{ and} \tag{1}$$

$$n_i = \sqrt{N_c N_v}\, e^{\frac{-E_g}{kT}} \tag{2}$$

where, N_c is the effective electron density of states in the conduction band, and N_v is the effective density of states in the valence band [19]. Obviously from (2), high temperature in a local region, whether caused by ions and/or defects will drive n_i up until (1) becomes true. Second breakdown occurs at this point through a microfilament path. Defects have been linked to the formation of microplasmas that can trigger a temperature rise that initiates second breakdown [18].

Silicon diodes experience the breakdown described by (1) and (2). In general, these devices will experience the aforementioned breakdown at very high reverse biases or under irradiation from high LET (>20 MeV.cm^2/mg) ions. Proton irradiation in silicon diode structures usually follows the behavior shown in Fig. 3. Reverse bias leakage current monotonically increases with fluence due to the generation of defects in the devices. No prompt failures are seen since the effective LET of a proton induced spallation reaction is not high enough to induce SEB. The failure mode is simply an overwhelming leakage current increase.

Silicon carbide reverse biased junctions under displacement damage inducing radiation will experience an increase in defects. The same irradiation should cause rare energy depositions that initiate the microplasmas that trigger the condition in (1) and (2). The combination of the damaged silicon carbide, which increase carrier generation sites and facilitates microplasma, and the charge collection from proton events should result in a breakdown event. This breakdown should occur under the following conditions: 1) high voltage to setup microplasma transport, 2) low LET hadron irradiation to cause displacement damage but not breakdown the device immediately, 3) and a critical defect density to provide a current path. This condition is mathematically described by percolation theory, which is mainly used in the description of breakdown in thin oxides in VLSI and ULSI devices [20]-[24].

Percolation theory in SiO_2 is similar to the reverse biased diode in that both have clearly segregated energy bands [20], [22]. Figure 4 depicts a possible condition for an ion assisted percolation failure of a device. After enough defects are induced by ions to almost make a circuit, a rare energy deposition from a proton, such as a spallation reaction, completes the circuit and provides enough liberated carriers to prime to circuit to initiate negative temperature coefficient breakdown. Since the percolation circuit also contains pre-irradiation defects like micropipes, these defects would reduce the number of radiation-induced defects required to complete the percolation circuit. And radiation induced defect generation is a stochastic process, so the distribution of breakdown voltages for the devices tested in this study will be broad. Figure 5 demonstrates this theoretical response. The current should rise with fluence at a constant reverse bias voltage, which is region 1. Region two is after a second breakdown occurs in the device due to increased defect population, enhancing microplasma injection from light ions to form the burnout path.

First order percolation theory reveals a useful prediction for breakdown damage levels even with the large noise margins that silicon carbide devices seem to have. First order percolation modeling is the most precise model that can be used since SiC devices have inherent variation in response. Since initial defect density is key for full application of percolation theory, which is not available for this study, a general model is presented here.

$$N_d = N_{d0}\left(1 - e^{-\sigma_t \Phi}\right) \tag{3}$$

is a statement of the generation rate of defects in the active region. N_d is the number of defects, N_{d0} is the maximum number of defects, and σ_t is the cross section for defect generation in the active region. The actual number of defects required for burnout is expected to be low, so the following approximation applies:

$$N_d = N_{d0}\sigma_t \Phi\,. \tag{4}$$

Percolation theory predicts breakdown will occur when an ion-induced microplasma completes a circuit of defects. The breakdown field will need to be higher if the

average distance between defects is large. This statement is essentially

$$V_{BD} = C\left(r_d^{ave}\right)^{\alpha}, \quad (4)$$

where V_{BD} is the breakdown voltage, C and α are constants, and r_d^{ave} is the average distance between defects. The average defect distance is related to the defect number by:

$$\frac{N_d}{N_{d0}} = \left(\frac{d_{SiC}}{r_d^{ave}}\right)^3 \quad (5)$$

where d_{SiC} is the lattice constant for silicon carbide. Combining (3) and (5) yields,

$$r_d^{ave} = d_{SiC}\left(\frac{1}{\sigma_t \Phi}\right)^{\frac{1}{3}}. \quad (6)$$

Inserting (6) into (4) then yields,

$$V_{BD} = C\left(\frac{d_{SiC}^3}{\sigma_t \Phi}\right)^{\frac{\alpha}{3}}. \quad (7)$$

The constants C and α will depend heavily on parameters such as dopant gradation, contact architecture and initial defect density. Unfortunately, this information is proprietary or unobtainable to this study, therefore the exact values of a C and α cannot be verified. Equation (7) should apply to both biased and unbiased irradiation, but the constants will change to accommodate the different average defect distance.

Since a high LET particles will deposit enough charge to set up the micorplasma event, the response will be similar to SEB in other power devices. That is, SEB will occur at a critical voltage at relatively low fluences. Therefore, reverse biased silicon carbide diodes should be seen to experience a SEB like breakdown under irradiation with high LET ions and experience a second breakdown event after a critical amount of low LET irradiation.

III. Procedure And Setup

The parts selected for this study were silicon carbide diodes from Cree, Inc. CSD01060 and CSD04060 are the part numbers. These are Schottky diodes that are available commercially.

For the primary measurement method, an HP4142 modular semiconductor measurement system was used with a 200 volt module (HP41420A), connected to the anode, and a single 1000 volt module (HP 411423A) was connected to the cathode. The HP4142 was connected to and controlled by a computer via a general-purpose instrument bus (GPIB). Electrical breakdown was defined as the voltage where the collector current (I_{CA}) reached the HP4142 current limit of 10^{-3}A. Electrical measurements were performed using the HP4142 source modular unit (SMU). Prior to irradiation all devices were characterized for forward voltage (V_f) and leakage current (I_{CA}) from anode to cathode.

To ensure that the testing method was not a factor in the breakdown of the device, a manual system was employed for a significant fraction of the proton testing. A discrete 1000V power supply was used to force a reverse bias while a DMM was used to measure leakage current. The leakage current could be measured by hand or captured through and RS-232 interface. In both test methods, the circuit impedance was keep low by using low impedance coaxial cables. The voltage drop seen across the cables was negligible.

The SEU test facilities at BNL provide a wide range of ions and energies for SEE testing. Crocker Nuclear Laboratory (CNL) of the University of California at Davis (UCD) has developed a facility to test radiation effects on photonic and electronic devices. The facility provides proton, deuteron and He-4 (alpha-particle) beams up to 68, 45, 90 MeV respectively. The devices all had active regions under 20 micrometers, so all the ions used in this study had constant LET over the device region. A list of ions used in this study is shown in Table II.

TABLE II.
IONS USED IN THIS STUDY.

Ion @ Energy	LET (MeV cm^2/mg)	Facility	Range in silicon (microns)
Protons @ 63 MeV	0.01	CNL	>1000
Lithium @ 99MeV	0.37	BNL	306
Fluorine @ 125 MeV	3.634	BNL	102
Bromine @ 210MeV	36	BNL	63.5
Iodine @ 329MeV	59.8	BNL	31.6

IV. Results

Since the variance of breakdown voltages of these devices is known to be large, a large number of devices were tested to ensure statistical significance. Tables III and IV list the statistical details of the study. For the proton tests, the variance in breakdown fluence was seen to converges on a limiting value when over 10 devices were tested. The variance in the breakdown voltage for heavy ions was very small due to the reproducible nature of the effect. Both of the methods of employing the HP4142 and the manual method reported equivalent results.

Proton irradiation did not affect the parts until prompt failure occured that is identical to second breakdown, i.e. high current and low voltage, as shown in Fig. 6. For fluences lower than 10^{15} cm^{-2}, breakdown did not occur for devices irradiated unbiased or biased lower than 400V when brought up to rated reverse bias, or 600V. This implies that the breakdown mechanism is due to the proton-induced events, such as spallation reactions, under bias coupled with a damaged substrate.

TABLE III.
DETAILS OF PROTON IRRADIATION – CSD1060

Reverse bias [V]	# of devices tested	Average Φ_{BD} [cm^{-2}]	Sigma of Φ_{BD} [cm^{-2}]
400	19	6E14	5.00E+14
500	17	2.32E13	1.00E+13
550	10	1E13	5.67E+12
600	24	5.1E12	5.03E+11

TABLE IV.
DETAILS OF HEAVY ION IRRADIATION – CSD1060

Ion species	SEB voltage range [V]	# of devices tested	Average Φ_{BD} [cm^{-2}]
Li	25	3	1.5E9
F	25	3	2.5E8
Br	50	2	2.65E5
I	50	2	5E5

Figure 6 compares well with the conceptual prediction of Fig. 5. The device experiences a catastrophic breakdown after a smaller increase in the leakage current. The device did not show a steady increase in current below the small jump at $7x10^{11}$ cm^{-2}. Current density may require a critical dose to increase significantly. Several technologies have shown a critical dose response [25], [26]. The jump in current before catastrophic failure is an anomaly. Most devices do not notably change in leakage current from proton irradiation.

To elucidate the intrinsic variance in the response of these devices, a test run of eight devices are shown in Fig. 7. Of these eight devices, one was irradiated at 600V reverse bias (Fig. 7a), three were irradiated at 500V (Fig. 7b), and four were irradiated at 550V (Fig. 7c). From these plots, the extreme variance in device parameters and response can be seen. Initial leakage current, slope of current increase with fluence, and the fluence at which breakdown occurs all have wide variation. This is not surprising considering the results shown in Fig. 2.

Figure 8 compares the initial leakage currents at 600V reverse bias for all of the CSD1060 devices tested in this study. Note that the abscissa is a log axis, which spans three orders of magnitude range in the values. There is no clear behavior to the distribution. The values were consistent between measurements before irradiations. To determine whether initial current correlates to breakdown voltage induced by radiation, the initial current and radiation induced breakdown fluence for irradiations at 500V and 600V are plotted on Fig. 9. Figure 9a shows the response in linear-linear scale, while Fig 9b. shows the log-linear response. No clear trend can be seen relating initial current to breakdown fluence.

From Fig. 9, a relationship between breakdown voltage and breakdown fluence can be seen. Devices irradiated at 600V breakdown at fluences one order of magnitude less proton fluence than devices irradiated at 500V. The relationship between breakdown voltage and breakdown fluence is plotted in Fig. 10. Most of the devices biased at 400V didn't breakdown, so the 400V point in Fig. 10 is a lower bound. This response agrees with the prediction of (7). Due to the variation of breakdown fluences of the parts measured, the one standard deviation errors bars in Fig. 10 are wide. The error bars are too wide to allow a confident extraction of the alpha constant, but alpha was seen to be in the range of two to three.

High LET particles reproducibly induced SEB at a critical voltage. The precision of the SEB critical voltage is listed in Table IV. The devices irradiated with ions with LETs over 10 MeV.cm^2/mg experience an SEB response at relatively low fluences. Figure 11 shows the relation between LET in silicon carbide and the breakdown voltage. The same data with NIEL in silicon carbide on the abscissa is shown in Fig. 12. There is a similar strong dependence on NIEL, which is similar to LET response. Both responses are typical of SEB responses seen for other power devices. In general, higher LET particles require less reverse bias and fluence to cause a breakdown event.

Breakdown voltage as a function of fluence is shown in Fig. 13, as opposed to total dose, which plotted in Fig. 14. Higher LET ions require less fluence to cause a breakdown event. Iodine and Bromine induced SEB at low fluences upon irradiation at the critical voltage of 325V. This indicates that SEB induced by heavy ions does not require pre-irradiation. Fluorine, Lithium, and protons require a significant amount of fluence to induce a breakdown event. Figure 14 depicts breakdown voltage vs. the product of fluence and NIEL. Obviously, much less accrued damage is needed to breakdown a device under high LET irradiation.

V. CONCLUSIONS

Silicon carbide Schottky diodes have shown unprecedented radiation sensitivity when reverse biased. Silicon carbide device are normally considered to be extremely robust to displacement damage inducing radiation, but the devices tested here show a unique failure mode that belies this trend. Similar effects were seen with reactor neutrons, which induce defects differently than the proton radiation used in this study. Clearly, device testing on silicon carbide devices will require an exception amount of control of manufacturing variables to remove the large variance present in the technology. Future studies will have to go beyond pin level testing, e.g., employing spreading resistance, resonance, and annealing measurements, to correlate breakdown parameters with innate device conditions.

VI. ACKNOWLEDGMENT

The authors would like to thank Mike Weideman, Dennis Thorbourne, and Tetsuo Miyahira of the Jet Propulsion Laboratory as well as Richard Harris and Martin Patton of Glenn Research Center.

VII. REFERENCES

[1] D.Braunig, D. Fritsch, B. Lehmann, A.L. Barry, 'Radiation-induced displacement damage in silicon carbide blue light-emitting diodes,' *Nuclear Science, IEEE Transactions on*, vol. 39, no. 3, pp. 428 – 430 June 1992.

[2] J.M. McGarrity, F.B. McLean, W.M. DeLancey, J. Palmour, C. Carter, J. Edmond, R.E. Oakley, "Silicon carbide JFET radiation response," *Nuclear Science, IEEE Transactions on*, vol. 39, no. 6, pp. 1974 - 1981 Dec. 1992.

[3] A.L. Barry, B. Lehmann, D. Fritsch, D. Braunig, "Energy dependence of electron damage and displacement threshold energy in 6H silicon carbide," *Nuclear Science, IEEE Transactions on*, vol. 38, no. 6, pp. 1111 – 1115 Dec. 1991.

[4] N. Mohan, T. M. Undeland, W. P. Robbins. *Power electronics: converters, applications, and design,* 3rd ed. Hoboken, NJ : John Wiley & Sons, c2003.

[5] A. Trzynadlowski, *Introduction to modern power electronics,* New York: Wiley, c1998.

[6] P. C. Sen, *Principles of electric machines and power electronics,* 2nd ed. New York : John Wiley & Sons, c1997.

[7] P.G. Neudeck, W. Huang, M. Dudley, "Study of bulk and elementary screw dislocation assisted reverse breakdown in low-voltage (<250 V) 4H-SiC p+-n junction diodes I. DC properties," *Electron Devices, IEEE Transactions on*, vol. 46, no. 3, pp. 478 - 484 March 1999.

[8] C.J. Scozzie, J.M. McGarrity, J. Blackburn, W.M. DeLancey, "Silicon carbide FETs for high temperature nuclear environments," *Nuclear Science, IEEE Transactions on*, vol. 43, no. 3, pp. 1642 - 1648 June 1996.

[9] J.M. McGarrity, C.J. Scozzie, J. Blackburn, W.M. Delancy, "High temperature silicon carbide FETs for radiation environments," *Nuclear Science Symposium and Medical Imaging Conference Record, 1995*, vol. 1, pp. 144 - 147 vol.1 21-28 Oct. 1995

[10] A. Ionascut-Nedelcescu, C. Carlone, A. Houdayer, H.J. von Bardeleben, J.-L. Cantin, S. Raymond, "Radiation hardness of gallium nitride," *Nuclear Science, IEEE Transactions on*, vol. 49, no. 6, pp. 2733 – 2738 Dec. 2002.

[11] J.M. McGarrity, F.B. McLean, W.M. DeLancey, J. Palmour, C. Carter, J. Edmond, R.E.Oakley, "Silicon carbide JFET radiation response," *Nuclear Science, IEEE Transactions on*, vol. 39, no. 6, pp. 1974 – 1981 Dec. 1992.

[12] F.B. McLean, J.M. McGarrity, C.J. Scozzie, C.W. Tipton, W.M. DeLancey, "Analysis of neutron damage in high-temperature silicon carbide JFETs," *Nuclear Science, IEEE Transactions on*, vol. 41, no. 6, pp. 1884 - 1894 Dec 1994.

[13] P.G. Neudeck, C. Fazi, "Study of bulk and elementary screw dislocation assisted reverse breakdown in low-voltage (<250 V) 4H-SiC p+-n junction diodes. II. Dynamic breakdown properties," *Electron Devices, IEEE Transactions on*, vol. 46, no. 3, pp. 485 – 492 March 1999.

[14] P. G. Neudeck, W. Huang, M. Dudley, And C. Fazi, "Non-Micropipe Dislocations In 4h-Sic Devices: Electrical Properties And Device Technology Implication," *MRS Symposium Proceedings* Volume 512, pp. 107-112.

[15] V. J.Nagesh, W. Farmer, R.F. Davis, and H.S. Kong, "Defects in neutron irradiated SiC," *Appl. Phys Lett*. 50(47), 27 April 1987.

[16] F. Gao and W. J. Weber, "Atomic-scale simulation of 50 keV Si displacement cascades in beta-SiC," Physical Review B, Vol. 63, p. 054101.

[17] R. Devanathan, W. J. Weber, and F. Gao, "Atomic scale simulation of defect prodection in irradiated 3C-SiC," Journal of Applied Physics, vol. 90, no. 5, pp. 2303-2309 2000.

[18] I. Kamata, H. Tsuchida, T. Jikimoto, K. Izumi, "A Comparative Study of the Electrical Properties of 4H-SiC Epilayers with Continuous and Dissociated Micropipes, "Silicon Carbide and Related Materials 2001**,** Materials Science Forum (Volume 389-393, pp. 1137-1140.

[19] A. Amerasekera, M.-C. Chang, J.A. Seitchik, A. Chatterjee, K. Mayaram, J.-H. Chern, "Self-heating effects in basic semiconductor structures," Elec*tron Devices, IEEE Transactions on*, vol. 40, no. 10, pp. 1836 – 1844 Oct. 1993.

[20] W. Kai, X. Hengkhun, and Ge. Jingpang, "Percolation and dielectric breakdown," *Proceedings of the 4th International Conference on Properties and Applications of Dielectric Commercials*, July 3-8, 1994, Brisbane Australia.

[21] R. Degraeve, G. Groeseneken, R. Bellens, J. L. Ogier, M. Depas, P. J. Roussel, and Herman E. Maes, "New insights in the relation between electron trap generation and the statistical properties of oxide breakdown," *Electron Devices, IEEE Transactions On*, Vol. 45, No. 4, April 1998.

[22] W. H. Lin, K. L. Pey, Z. Dong, S. Y. M. Chooi, C. H. Ang, J. Z. Zheng, "The Statistical Distribution of Percolation Current for Soft Breakdown in Ultrathin Gate Oxide," 336 *IEEE Electron Device Letters*, Vol. 24, No. 5, May 2003.

[23] M. A. Alam, B. E. Weir, P. J. Silverman, "A Study of Soft and Hard Breakdown—Part I: Analysis of Statistical Percolation Conductance," *IEEE Transactions On Electron Devices*, Vol. 49, No. 2, February 2002

[24] S. S. Sombra, U. M.S. Costa, V. N. Freire, E.A. de Vasconcelos, E. F. da Silva Jr. "A percolation based dielectric breakdown model with randomic changes in the dielectric constant," *Physica A* 305 (2002) 351 – 359.

[25] V. Ferlet-Cavrois, S. Quoizola, O. Musseau, O. Flament, J.L. Leray, J.L. Pelloie, C. Raynaud, O.Faynot, "Total dose induced latch in short channel NMOS/SOI transistors," *Nuclear Science, IEEE Transactions on*, vol. 45, no. 6, pp. 2458 – 2466 Dec. 1998.

[26] F.W. Sexton, D.M. Fleetwood, M.R. Shaneyfelt, P.E. Dodd, G.L. Hash, L.P. Schanwald, R.A. Loemker, K.S. Krisch, M.L. Green, B.E. Weir, P.J. Silverman, "Precursor ion damage and angular dependence of single event gate rupture in thin oxides," *Nuclear Science, IEEE Transactions on*, vol. 45, no. 6, pp. 2509 – 2518 Dec. 1998.

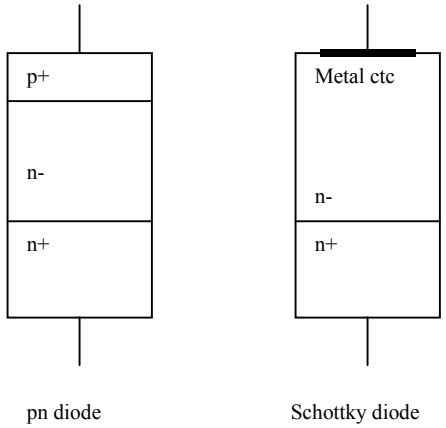

Fig. 1. Pn and Schottky diode structures.

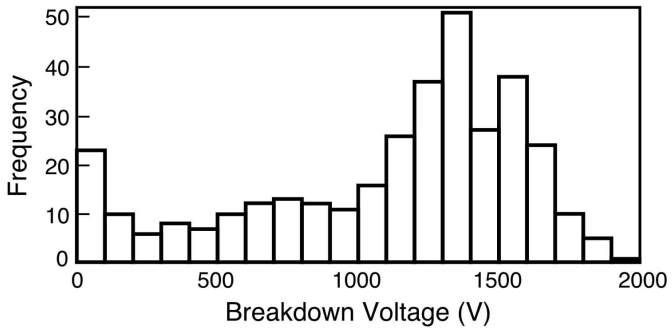

Fig. 2. Distribution of breakdown voltages in micropipe free Schottky barrier diodes. Taken from [18].

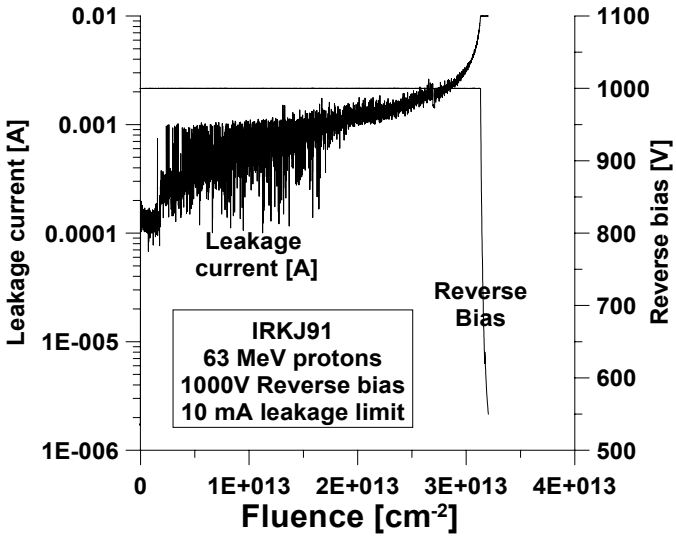

Fig. 3. Response of a silicon power diode to 63 MeV protons. The response is typical of leakage induced by defects, i.e., leakage increase with fluence with no prompt SEE effects. Device was biased at 1000V.

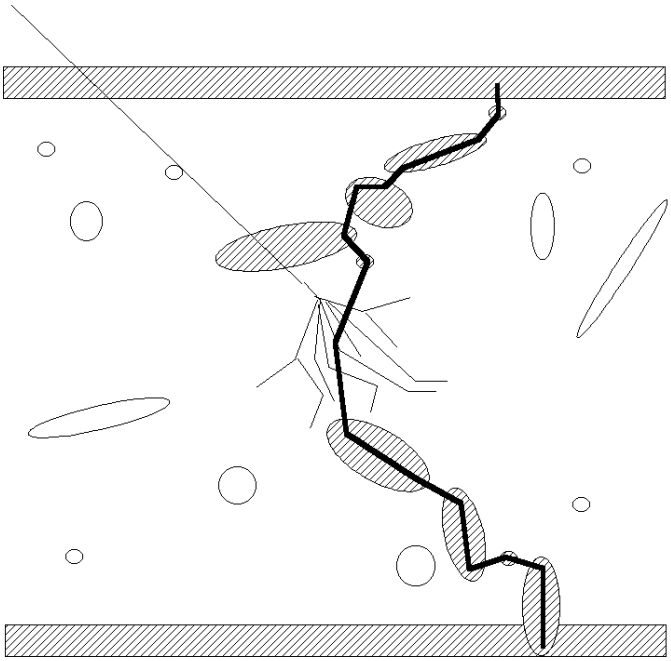

Fig. 4. Depiction of how a circuit of defects can initiate a prompt breakdown. Random injection of conductive defects is described by percolation theory. Conductive defects can be radiation induced defects or clusters, screw defects or micropipes, or stacking faults. A rare radiation event, like a spallation reaction, primes the circuit to allow second breakdown.

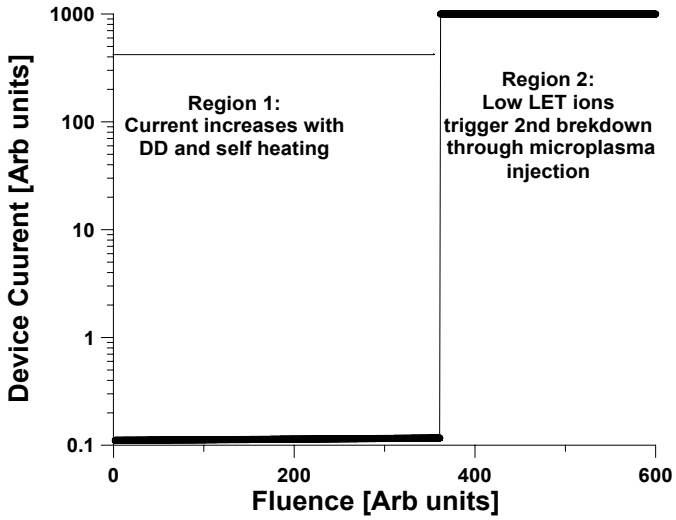

Fig. 5. Postulated response of a silicon carbide Schottky diode to low LET fluence. The prompt failure is due to the completion of the percolation circuit triggered by a microplasma injection from a rare proton event.

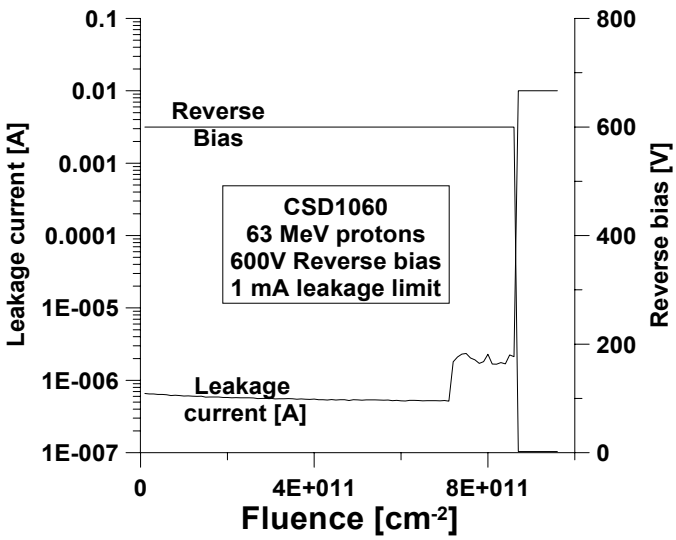

Fig. 6. Response of a silicon carbide Schottky CSD1060 diode to proton dose. Device was biased at 600V. Unlike silicon devices, the leakage current down not in general increase with fluence, but actually decreases until single events occur. Breakdown does not occur when the device is irradiated unbiased and then biased until much higher fluences.

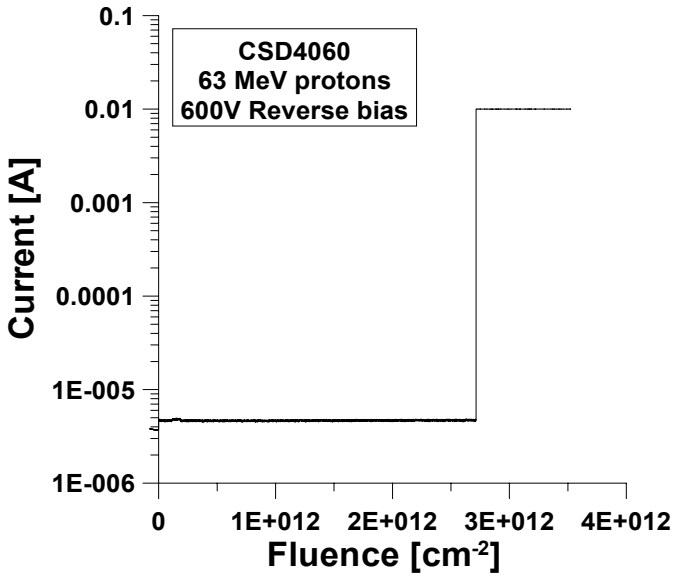

Fig. 7a. Response of a silicon carbide Schottky CSD4060 diode to proton fluence. Device was biased at 600V. The leakage current does not change during irradiation before the prompt failure.

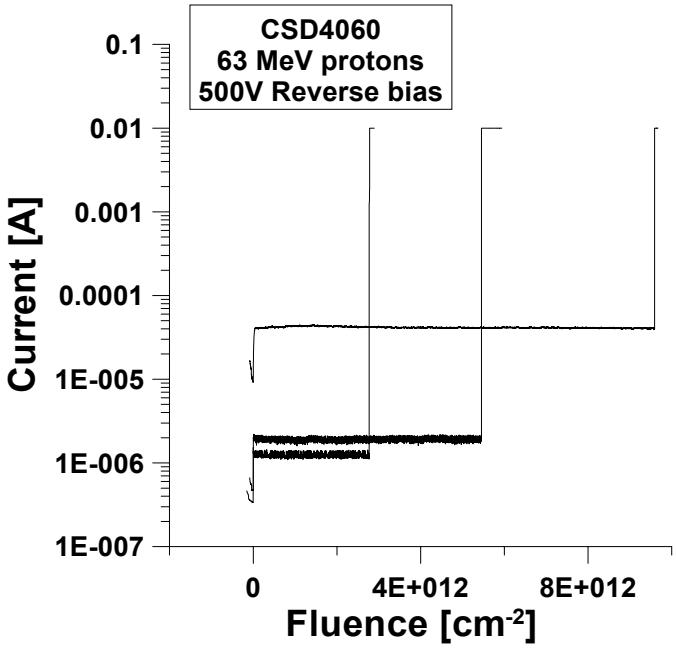

Fig. 7b. Response of a silicon carbide Schottky CSD4060 diode to proton fluence. Device was biased at 500V.

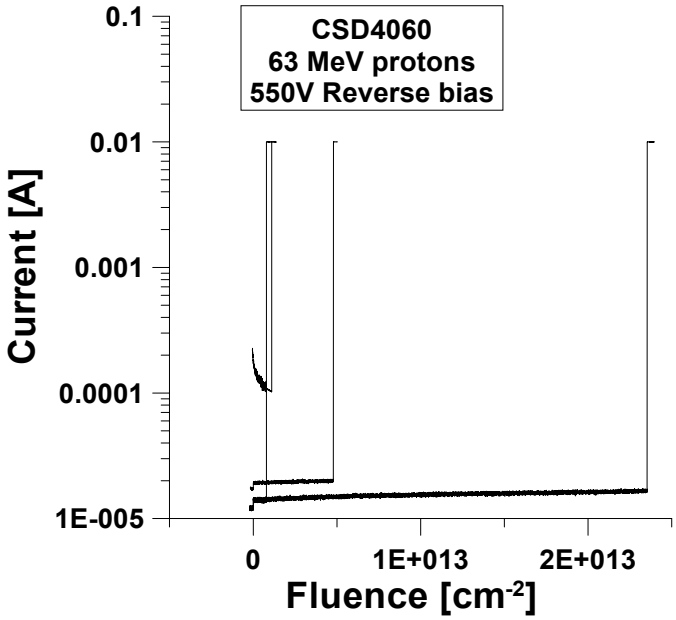

Fig. 7c. Response of a silicon carbide Schottky CSD4060 diode to proton fluence. Device was biased at 550V.

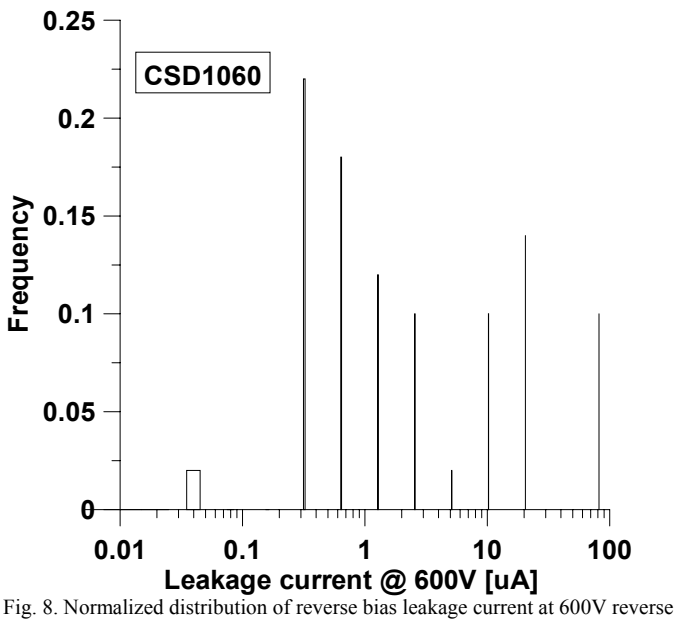

Fig. 8. Normalized distribution of reverse bias leakage current at 600V reverse bias. The parts tested in this study experiences variance of over three orders of magnitude. Fifty one parts make up this population.

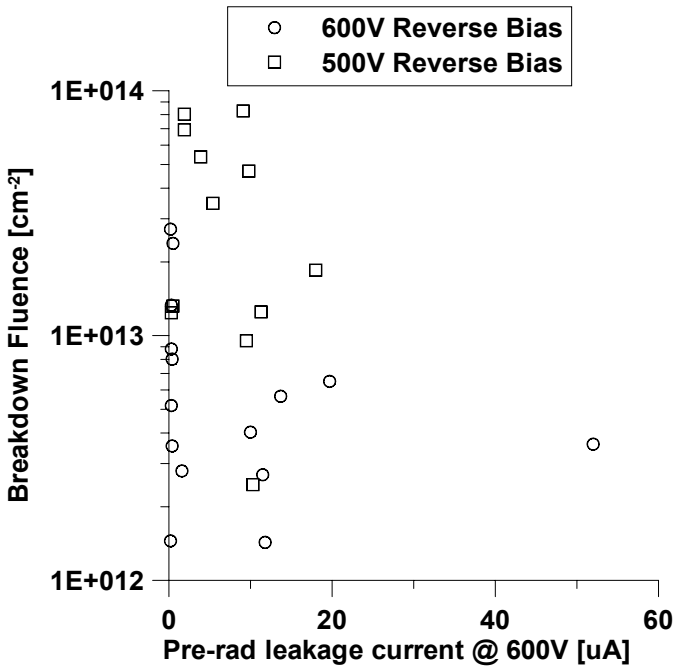

Fig. 9a. Scatter plot of the fluence at which breakdown occurred versus the pre-irradiation leakage current. No trend is obvious except that the irradiation at 600V correlated to a breakdown fluence one magnitude less than irradiations are 500V reverse bias.

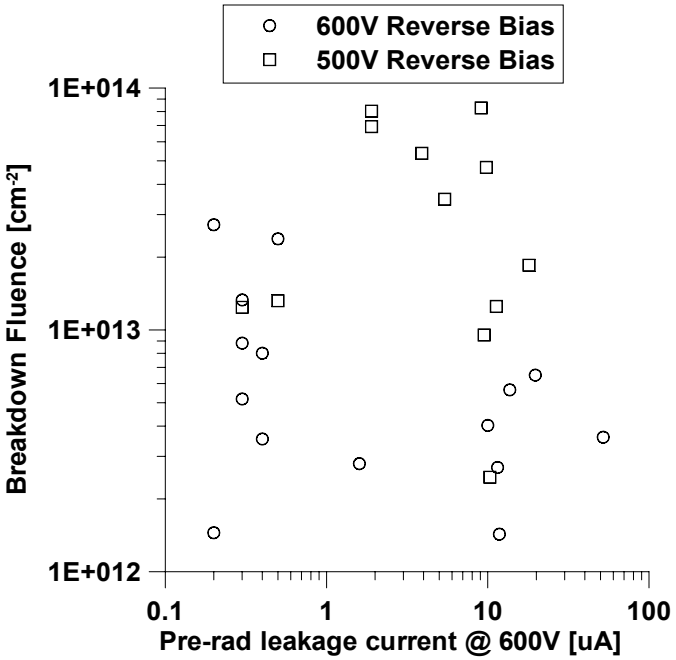

Fig. 9b. Scatter plot of the fluence at which breakdown occurred versus the pre-irradiation leakage current. No trend is obvious except that the irradiation at 600V correlated to a breakdown fluence one magnitude less than irradiations are 500V reverse bias.

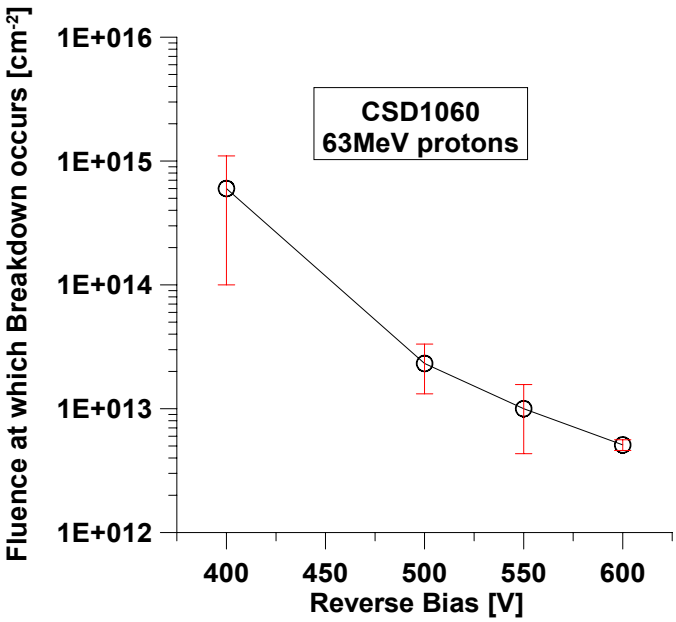

Fig. 10 Mean Fluences for prompt failure of csd1060 versus reverse bias voltage. Error bars are the standard deviation for fluences required for prompt failure for each bias condition. Due to the large inherent variance in the breakdown voltages of the devices, the error bars are quite large but a trend is evident.

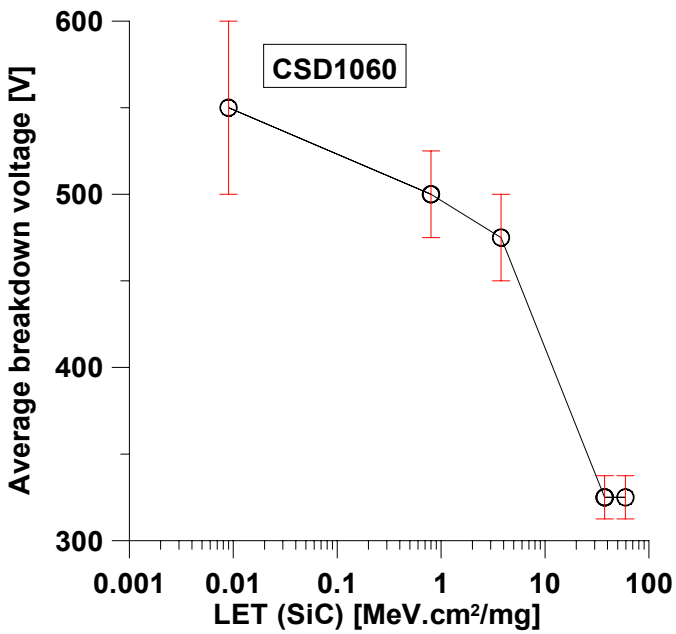

Fig. 11. Voltage at which a silicon carbide diode experiences destructive breakdown as a function of LETs of different ions. The device begins to experience immediate SEE type effects at LETs over 10 MeV-cm^2/mg.

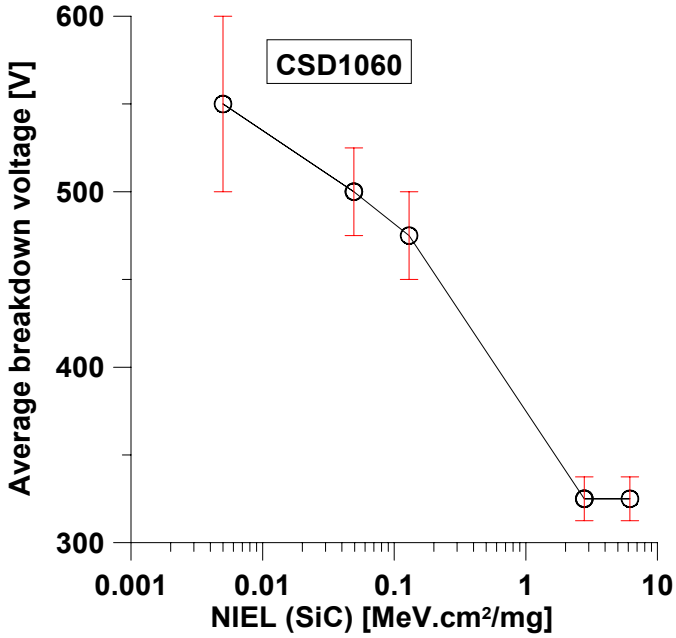

Fig. 12. Voltage at which a silicon carbide diode experiences destructive breakdown as a function of NIELs of different ions.

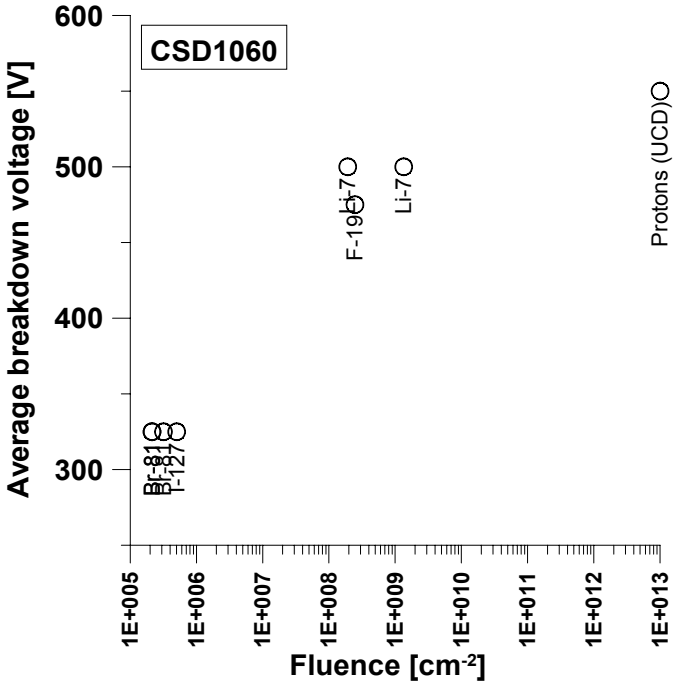

Fig. 13. Voltage at which a silicon carbide diode experiences destructive breakdown as a function of particle fluence.

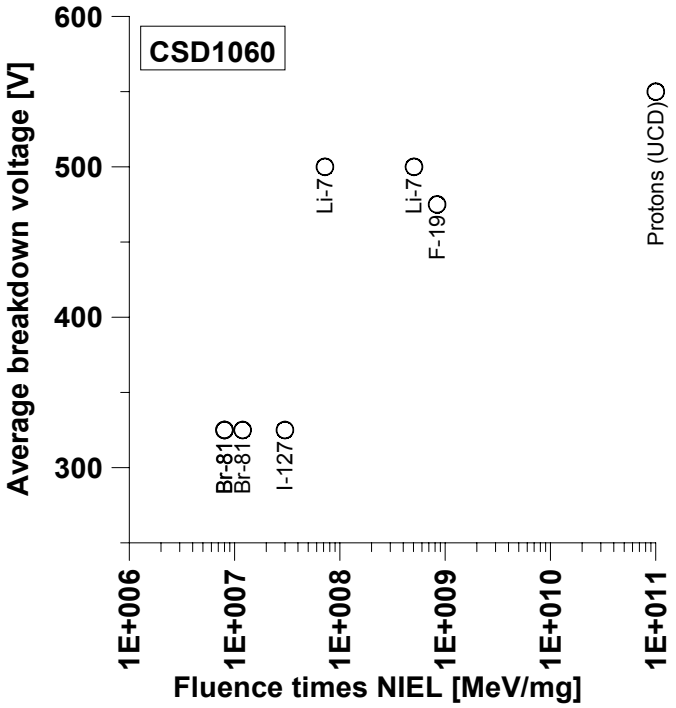

Fig. 14. Voltage at which a silicon carbide diode experiences destructive breakdown as a function of the product of the fluence and NIEL.